Monte Carlo method for evaluation of surface emission rate measurement uncertainty

Yuan-Qiao Li,[1, *] Min Lin,[1, 2] Li-Jun Xu,[1, 2] Rui Luo,[1, 2] Yu-He Zhang,[1, 2] Qian-Xi Ni,[3, 4, †] and Yun-Tao Liu[1, 2]

[1]*China Institute of Atomic Energy, Beijing 102413, China*
[2]*National Key Laboratory for Metrology and Calibration Techniques, Beijing 102413, China*
[3]*Department of Radiation Oncology, Hunan Cancer Hospital, Changsha 410031, China*
[4]*The Affiliated Cancer Hospital of Xiangya School of Medicine, Central South University, Changsha 410031, China*

The aim of this study is to evaluate the uncertainty of $2\pi\alpha$ and $2\pi\beta$ surface emission rates using the windowless multiwire proportional counter method. This study used the Monte Carlo method (MCM) to validate the conventional Guide to the Expression of Uncertainty in Measurement (GUM) method. A dead-time measurement model for the two-source method was established based on the characteristics of a single-channel measurement system, and the voltage threshold correction factor measurement function was indirectly obtained by fitting the threshold correction curve. The uncertainty in the surface emission rate was calculated using the GUM method and the law of propagation of uncertainty. The MCM provided clear definitions for each input quantity and its uncertainty distribution, and the simulation training was realized with a complete and complex mathematical model. The results of the surface emission rate uncertainty evaluation for four radioactive plane sources using both methods showed an uncertainty consistency $E_{\rm n} < 0.070$ for the comparison of each source, and the uncertainty results of the GUM were all lower than those of the MCM. However, the MCM has a more objective evaluation process and can serve as a validation tool for GUM results.

Keywords: Surface emission rate, Uncertainty, Monte Carlo method, Metrology, Probability distribution function, Dead time, Low-energy loss correction, Least-squares method

I. INTRODUCTION

Spills, leaks from unsealed sources, or breakage or breach of the integrity of sealed sources can result in radioactive contamination of material surfaces. This requires the effective monitoring of surface radioactive contamination in radiation workplaces. Large-area α- and β-plane sources are widely used to provide the necessary traceability for measurements [1–5]. For absolute measurements of α and β surface emission rates, large-area windowless multiwire gasflow proportional counter systems are commonly used. In this approach, the measurement function of the surface emission rate E is modeled as follows [6–9]:

$$E = \frac{R}{1 - \tau R} f - B \tag{1}$$

where R is the particle count rate, B is the background count rate, τ is the dead time of the counting system, and f is the correction factor. R and B can be obtained by direct measurement. However, for the system dead time τ and correction factor f, there are differences in the measurement models obtained using different measurement instruments and methods.

The conventional approach to the evaluation of surface emission rate uncertainty is the Guide to the Expression of Uncertainty in Measurement (GUM) method [10], which uses a nonlinear functional model to propagate uncertainty. This method determines the combined standard uncertainty of the output quantities using the law of uncertainty propagation. In the measurement function model of the surface emission rate E, the standard uncertainties of R and B are obtained

by statistically determining the experimental standard deviation of the measured values, a process known as Type A evaluation of uncertainty. For counting measurement systems based on single-channel analysis techniques, the system dead time τ is typically obtained using the two-source measurement model, and the correction factor f is typically referred to as the voltage threshold correction factor f_d. The value of f_d is obtained by fitting the threshold extrapolation curve using the low-energy correction method. These two evaluation processes are usually classified as Type B uncertainty evaluations. This is due to the fact that when evaluating the uncertainty of surface emission rate using the GUM method, calibrators often make artificial assumptions about the probability distribution of measurement results from complex nonlinear equation models, usually assuming a rectangular distribution, and the effect of this method on the uncertainty evaluation results is unknown.

Owing to the nonlinear nature of the measurement model and the challenges associated with calculating the partial derivatives of the model in the surface emission rate uncertainty, the uncertainty can be measured using the Monte Carlo method (MCM) proposed in ISO/IEC GUIDE 98-3 [11]. As shown in Fig. 1, the MCM obtains the probability distribution function (PDF) of the output quantity Y by randomly sampling the PDF of the input quantity X_i. On this basis, the best estimates of output quantity, standard uncertainty, and coverage interval are obtained.

The MCM has been used less frequently in uncertainty assessment studies of nuclear measurements [12, 13]. This is due to the fact that, although the GUM method has a generalized law of propagation of uncertainty, a complete and specific measurement function model may differ due to the variations in experimental measurements for each measured quantity and the differences in function models for each component, resulting in a complex law of propagation of uncertainty with Taylor expansions. The staff may intentionally
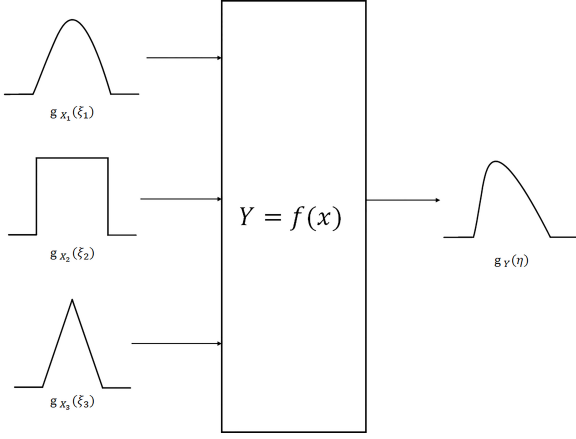
Fig. 1. Description of evaluation uncertainty by the Monte Carlo method (MCM). The probability distribution of the input quantity X_i involves the normal distribution $gx_1(\xi_1)$, rectangular distribution $gx_2(\xi_2)$, triangular distribution $gx_3(\xi_3)$, among others, and the probability distribution $g_Y(\eta_1)$ of the output Y is unknown.

simplify the measurement model through known evaluation results, avoid complex terms in the evaluation process, or treat them as constants to regain uncertainty with a smaller value, which may affect the accuracy of the traceability of quantity values [14]. In contrast, the MCM can directly perform calculations for a variety of complex models to obtain the best estimate and standard uncertainty without considering the trade-offs between higher-order terms of the Taylor expansion in the law of the propagation of uncertainty. Therefore, the key to the MCM is to obtain a model of the function between the input and output quantities and its probability distribution for each measured quantity.

To evaluate the $2\pi\alpha$ and $2\pi\beta$ surface emission rate uncertainties, this study first describes the experimental setup, measurement method, and model for the system dead time and voltage threshold correction factor. The MCM is used to refine the surface emission rate measurement function model based on Eq. 1. Finally, the law of propagation of the uncertainty of the GUM is verified and compared with the functional model of the MCM.

II. METHODS

1. Experimental set-up

In this study, a large-area windowless multiwire gas-flow proportional counter [15] developed by the China Institute of Atomic Energy (CIAE) was used as the detector. The working principle of this detector is based on the primary ionization of α and β particles in the sensitive volume of the proportional counter, which produces positive ions and electrons. These particles are then accelerated by an electric field to gain sufficient energy to trigger secondary ionization with gas molecules. The number of electron–ion pairs produced by this process is proportional to the number of electron–ion

pairs produced by the primary ionization, resulting in a linear amplification of the primary ionization pulse signals from the α and β particles.

For the single-channel counting measurement requirements of this experiment, the electronic equipment included a high-voltage DC power supply, current-type pre-amplifier, pulse-shaping circuit, timing single-channel analyzer, monostable control unit, and timer/counter. A diagram of the instrument is shown in Fig. 2. P-10 gas (a mixture of 90% Ar and 10% CH_4) was used as the operating gas at a flow rate of 100 mL/min. The working high voltage for the α-plane source was 2100 V, whereas that for the β-plane source was 2800 V. Measurements were performed on four plane sources (^{241}Am, ^{238}Pu, ^{90}Sr, and ^{204}Tl). According to oscilloscope observations, the pulse width of the pulse signal output from the main amplifier was generally less than $2\,\mu s$. The output pulse width of the single-channel analyzer was approximately 650 ns, whereas the pulse width of the monostable control unit had an adjustable range of 0.4–4 μs.

2. Dead time measurement

The surface emission rate of plane sources generally does not exceed 5000 s^{-1}, resulting in a dead time that produces leakage counts that may have a small effect on the count rate measurements [16–22]. However, because the windowless proportional counter is an absolute measurement device, it is necessary to measure the dead time of the system to correct for leakage counts. The dead time provided by the monostable control unit within the measurement system is a non-extended dead time; however, the system dead time is also affected by various components. Therefore, it is necessary to measure the system dead time experimentally. ICRU Report 52 [23] recommends three methods for measuring the dead time. In this experiment, a two-source two-pulse method was used to measure the dead time of the system. In this method, pulse signals are generated from two different radioactive sources and input into the detector separately to obtain the measurement count rates of the two sources, n_1 and n_2. The two sources are then measured simultaneously using a detector to obtain the mixed measurement count rate n_{12}. Ideally, the real count rate of three sets of pulse count rates n'_1, n'_2, and n'_{12} should satisfy $n'_1 + n'_2 = n'_{12}$, and according to the formula for the real count rate of a non-extended dead time system, $n' = n/(1 - \tau n)$, the dead time formula for the two-source method is finally obtained:

$$\tau = \frac{n_1 + n_2 + n_{12}}{2n_1 n_2}. \tag{2}$$

3. Threshold correction factor measurements

To avoid the influence of noise on count measurement, a discriminating voltage threshold must be set. Because the energy of α particles is high and the discriminating threshold
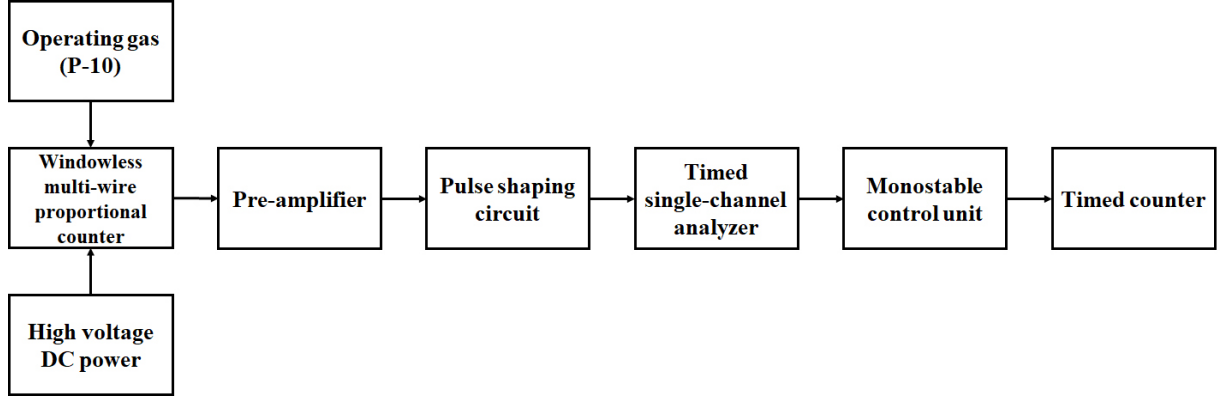
Fig. 2. Actual size of a well-prepared line drawing.

is set low, small changes in the α-particle count rate measurement can be ignored. However, the energy spectrum of β sources is continuously distributed, and it is difficult to distinguish their low-energy signal from noise signals using the pulse amplitude. Consequently, setting the discriminating voltage threshold may result in a loss of the β-particle count rate, and a threshold correction for β sources must be performed [5, 24–26].

Some National Metrology Laboratories [27, 28] that use multichannel analyzers to construct measurement systems typically calibrate the site corresponding to the lower threshold by using 10% of the site of the ^{55}Fe full-energy peak. This is primarily designed to correct for count-rate variations owing to fluctuations in the gain of the working gas. Although a measurement system based on a single-channel analyzer cannot set a lower threshold by determining the absolute energy, it is possible to set different lower discriminating voltage thresholds to obtain the count rate at different discriminating voltage thresholds, and then extrapolate to obtain the count rate when the threshold is zero.

The threshold extrapolation curves are influenced by low-energy noise interference and the characteristics of the beta smooth continuum spectrum and can only be assumed to be a straight line over a small threshold interval. As a rule of thumb, the normalized value (predicted value/fitted intercept) of the fitted curve should not exceed 90%. The threshold extrapolation curve fitted using the least-squares method [29–33] is a straight line, where x represents the voltage threshold and y represents the measured count rate. The equation for the fitted curve is as follows:

$$y = px + q, \tag{3}$$

where p and q represent the slope and intercept of the line, respectively. This equation is solved as follows:

$$p = \frac{j\sum x_i y_i - (\sum x_i)(\sum y_i)}{n\sum x_i^2 - (\sum x_i)^2}, \tag{4}$$

$$q = \frac{(\sum x_i^2)(\sum y_i) - (\sum x_i y_i)(\sum y_i)}{j\sum x_i^2 - (\sum x_i)^2}, \tag{5}$$

where $i = 1, 2, \ldots, j$. To fit a straight line, a minimum of $j = 5$ measurements must be substituted into the equation to complete the fit with degrees of freedom $\nu = j - 2$.

4. Evaluation by the GUM method

The evaluation process of the GUM method is divided into two types of evaluations: A and B. This study focuses on two uncertainty components: system dead time and voltage threshold correction factor, and the process is a Type B evaluation. The uncertainty obtained from the Type B evaluation of uncertainty can be obtained using Eq. (6).

$$u_{\mathrm{B}} = a/k = \max(\Delta a)/k, \tag{6}$$

where a represents the half-width of the interval of the possible measurement values, or the maximum fluctuation $\max(\Delta a)$ if the coverage interval distribution is asymmetric [6, 34], and k is the coverage factor. Therefore, obtaining the coverage interval and probability distribution of the components is crucial.

a. Evaluation of system dead-time uncertainty In the GUM method, the monostable control unit produces a square wave as the output signal. The pulse width of this signal is typically measured using an oscilloscope, which requires debugging the oscilloscope's resolving power and sampling time interval. After debugging, the system dead-time interval half-width a is determined based on the time interval of the index value, as shown on the oscilloscope. Because the probability distribution function of the system's dead time is unknown, it is generally assumed that the error follows a rectangular distribution, in which case $k = \sqrt{3}$.

b. Evaluation of voltage threshold correction factors uncertainty In this study, the threshold correction curves were fitted using the least-squares method. The expected corrections obtained from the calibration curves and their standard uncertainties were calculated using their intercepts, slopes, estimated variances, and covariances. Multiple sets of thresholds and the corresponding measurements were selected and

substituted into Eqs. 4 and 5 to obtain the p and q values, which were substituted into the following equation:

$$s^2 = \frac{\sum(y_i - px_i - q)^2}{j - 2} \qquad (7)$$

$$s^2(p) = \frac{js^2}{j\sum x_i^2 - (\sum x_i)^2} \qquad (8)$$

$$s^2(q) = \frac{s^2 \sum x^2}{j\sum x_i^2 - (\sum x_i)^2} \qquad (9)$$

$$r(p,q) = \frac{-\sum x_i}{\sqrt{j\sum x_i^2}} \qquad (10)$$

where $s(p)$ is the standard deviation of the slope, $s(q)$ is the standard deviation of the intercept, s^2 is the estimated variance of the fitted curve, and $r(p,q)$ is the correlation coefficient between the p and q estimates. This provided the combined standard uncertainty [10] of the measured count rate (y) corresponding to the specified prediction threshold (x) on the fitted curve.

$$u_c^2(y) = u^2(q) + x*u^2(p) + 2x*u(p)*u(q)*r(p,q) \quad (11)$$

The coverage interval [35, 36] for each measured count rate on the fitted curve was obtained as $[px_i + q + u_c(y_i), px_i +$

$q + u_c(y_i)]$. In addition, because y_i is an experimental measurement, and the result of $(px_i + q)$ is the predicted value of the fitted curve, the voltage threshold correction factor f_d is expressed as follows:

$$f_d = \frac{q}{px + q} \qquad (12)$$

This yields an asymmetric coverage interval for f_d: $[\frac{q}{px+q+u_c(y)}, \frac{q}{px+q-u_c(y)}]$. According to the GUM, because the probability distribution function of f_d is unknown, its coverage interval distribution is assumed to be rectangular by default. According to Equation (7), the uncertainty components of the voltage threshold correction factors are obtained as follows:

$$u(f_d) = \frac{\max(\frac{q}{px+q-u_c(y)} - \frac{q}{px+q}, \frac{q}{px+q} - \frac{q}{px+q+u_c(y)})}{\sqrt{3}} \qquad (13)$$

c. Evaluation of the combined standard uncertainty
The previous two subsections provide the system dead-time and voltage threshold correction factors and their uncertainty components, which can be used to obtain the relative uncertainty of each component. According to the GUM method, the relative combined standard uncertainty $u(E)$ of the surface emission rate can be derived from Eq. 1 using the law of propagation of uncertainty proposed by Stanga [37].

$$u(E) = \frac{(E+B)^2}{RE}\sqrt{u^2(R) + \frac{R^2}{(E+B)^2}u^2f_d + \tau^2R^2u^2(\tau) + u^2(B)\frac{R^2B^2}{(E+B)^4}} \qquad (14)$$

Here, R and B belong to the Type A evaluation of uncertainty, both of which were obtained from experimental measurements. $u(R)$, $u(B)$, $u(f_d)$, and $u(\tau)$) are the relative standard deviations of R, B, f_d, and τ, respectively.

5. *Evaluation by the MCM*

The MCM provides a general numerical approach for evaluating the measurement uncertainty for models with any number of input quantities that can be characterized by a PDF and a single output quantity. In this study, MATLAB was used as the Monte Carlo simulation platform to model the measurement between the output quantities Y and input quantities $X_1, \ldots, X_N$. According to Equations (1), (2), and (12), a new measurement function for the surface emission rate E can be obtained as follows:

$$E = \frac{R}{1 - \frac{n_1 + n_2 - n_{12}}{2n_1n_2}R}\frac{q}{px+q} - B \qquad (15)$$

The probability distributions, best estimates, standard uncertainties, and coverage intervals of the propagated input quantities X_i for each measurement model were analyzed. The probability distributions for each input quantity are listed in Table 1.

Finally, the estimated and standard uncertainty of Y were calculated from the PDF of Y and the coverage interval of Y at a 95% coverage probability (k=2).

III. RESULTS

The order of the experimental measurement was as follows: first, the system dead time was measured, then the voltage

TABLE 1. Information on model propagation inputs for the MCM of measurement.

Input (X_i)	Sources of data	Probability distribution
R	Experimental measurement results	Normal
B	Experimental measurement results	Normal
n_1	Experimental measurement results	Normal
n_2	Experimental measurement results	Normal
n_{12}	Experimental measurement results	Normal
x	Experimental scale readings	Rectangular
p	Calculated results	Normal
q	Calculated results	Normal

threshold correction factor was determined, followed by the count rate and background, and finally, the combined standard uncertainty was calculated.

1. GUM method

a. System dead time uncertainty The system dead-time measurements were performed using two α-plane sources with a count rate of 5000 s^{-1}. Ten measurements were taken per set of experiments, and the statistical standard deviations obtained as the measurement uncertainties are listed in Table 2.

The measured values in Table 2 were substituted into Eq. (2) to obtain the system dead-time values. According to the method described in Section 2.4.1, the half-widths of the interval of the system dead time, $a= 0.2\,\mu$s, and $k = \sqrt{3}$, are used to obtain the uncertainty of the measurement of the system dead time, as presented in Table 3.

b. Voltage threshold correction factor uncertainty The threshold correction curves of the ^{90}Sr and ^{204}Tlplane sources were measured by increasing the threshold voltage from 0.040 V. The measured count rate at each set of voltages was recorded, and the obtained data are shown in Figures 3 and 4.
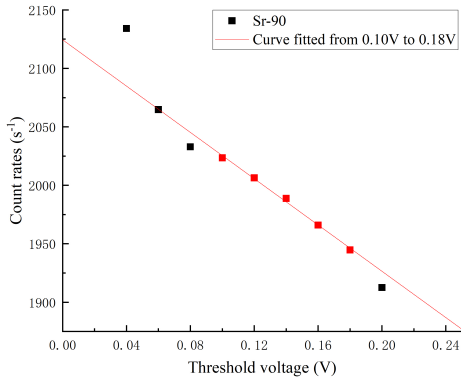

Fig. 3. The coordinate plots of β-source (^{90}Sr) show eight coordinate points, and five coordinate points from 0.10 to 0.18 V were used for curve fitting, with the fitted coordinate points and fitted straight line marked in red.

Fig. 4. The coordinate plots of β-source (^{204}Tl) show eight coordinate points, and five coordinate points from 0.10 to 0.18 V were used for curve fitting, with the fitted coordinate points and fitted straight line marked in red.
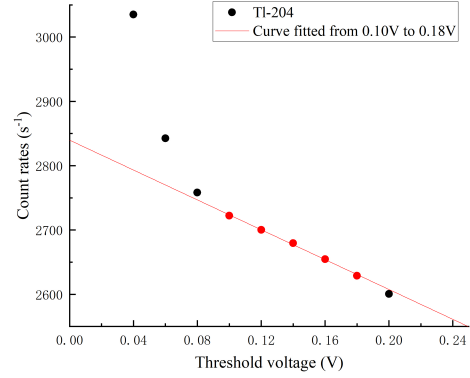
According to the threshold correction curve plots of the ^{90}Sr and ^{204}Tl plane sources, the following was found: at 0.04 to 0.10 V, the curve non-linearity fluctuated greatly, mainly because the count rate contained a large number of noise signals; at 0.10 to 0.18 V, the correlation coefficient of the fitted curves had the largest value of R^2, the fitting effect was the best, and the normalized values of the count rate (predicted value/fitted intercept) were all greater than 90%. The normalized curve obtained is shown in Figure 5. The above five sets of measurements were then entered into Equations (4) and (5), and the slopes p and intercepts q of the threshold correction curves for the ^{90}Sr and ^{204}Tlplane sources, as well as the standard deviation $s(p)$ of the slopes, the standard deviation $s(q)$ of the intercepts, the estimated variances s^2, and the correlation coefficients $r(p, q)$, were obtained and recorded in Table 4.

By substituting the calculation results in Table 4 into Equation (11), the uncertainty was evaluated for five sets of data in the range of 0.10 to 0.18 V, and the results are listed in Table 5.

Both relative standard uncertainties of the two β sources are minimized at the threshold $x = 0.10$ V. By substituting the predicted values at this threshold into Equation (12), the voltage threshold correction factors and coverage intervals for the two sources were obtained, as shown in Table 6.

TABLE 2. Dead time measurement results of two-source method.

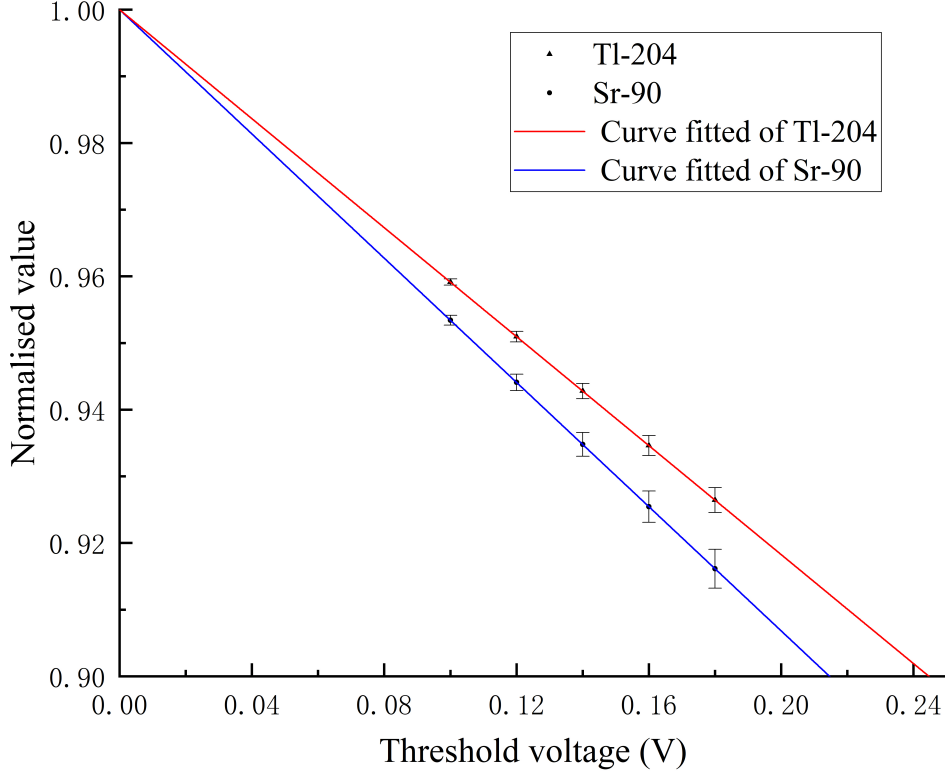| Quantity of experiments	Measured value (s^{-1})	Standard deviation (s^{-1})
$n_1(^{239}\text{Pu})$	5229.78	26.10
$n_2(^{241}\text{Am})$	5403.96	12.61
$n_{12}(^{239}\text{Pu} +^{241}\text{Am})$	10424.83	27.79

Fig. 5. Threshold extrapolation straight line for two β sources where the counting rates have completed normalization, including error bars for each predicted value on the fitted line.

TABLE 3. System dead time and its uncertainties with the GUM method.

System dead time (s)	Standard uncertainty (s)
3.696×10^{-6}	0.115×10^{-6}

The voltage threshold correction factors and uncertainties for the two β sources were then obtained from Equation (13), as listed in Table 7.

c. Combined standard uncertainty The measured data were collated when the α source did not require threshold correction by setting its f_d value to 1 and its $u(f_d)$ value to 0. The results are summarized in Table 8.

By substituting various data from Table 8 into Equation (14), the standard and relative standard uncertainties of the four plane sources were obtained, as listed in Table 9.

2. Monte Carlo method (MCM)

According to the information in Table 1, the input quantity X_i for the Monte Carlo simulation was defined as follows: The input quantities (n_1, n_2, n_{12}) and their normal distributions for the system dead time were obtained from Table 2. The standard deviations of p and q were obtained from Equations (8) and (9) and were assumed to be normally distributed by default. The threshold voltage reading $x = 0.10$ V had a rectangular distribution with a scale component value of 0.02 V, and its coverage interval was set to [0.08, 0.12]. The measurements of count rate R and background count rate B in Table 6 were used to obtain the coverage interval of the normal distribution of these two quantities using their standard deviations. In the Monte Carlo simulation, the random sample size for each input quantity was set to $M = 10^7$. The uncer-

TABLE 4. Parameters of threshold correction curves for two β sources.

β sources	p	q	$s(p)$	$s(q)$	s^2	$r(p,q)$
^{90}Sr	-989.76	2124.44	61.69	5.09	5.07	-0.98020
^{204}Tl	-1160.56	2839.67	52.89	4.36	3.73	-0.98020

TABLE 5. Standard uncertainties of five sets of predicted values on the threshold correction curves for the two β sources

Coordinate	Threshold /V	^{90}Sr		^{204}Tl	
		Standard deviation (s^{-1})	Relative standard deviation	Standard deviation (s^{-1})	Relative standard deviation
x_1	0.10	1.554	0.08%	1.332	0.05%
x_2	0.12	2.618	0.13%	2.244	0.08%
x_3	0.14	3.787	0.19%	3.246	0.12%
x_4	0.16	4.987	0.25%	4.275	0.16%
x_5	0.18	6.200	0.32%	5.315	0.20%

tainties for the system dead time, β-source voltage threshold correction factors, and combined standard uncertainty were obtained, and the results are presented in Tables 10, 11, and 12.

A normalized histogram of the distribution function of the system dead time obtained by the Monte Carlo simulation is shown in Figure 6. A normalized histogram of the distribution function of the voltage threshold correction factors for the two β sources is shown in Figure 7. A normalized histogram of the distribution function of the surface emission rate for the four sources is shown in Figure 8. Each histogram contains 200 bars.
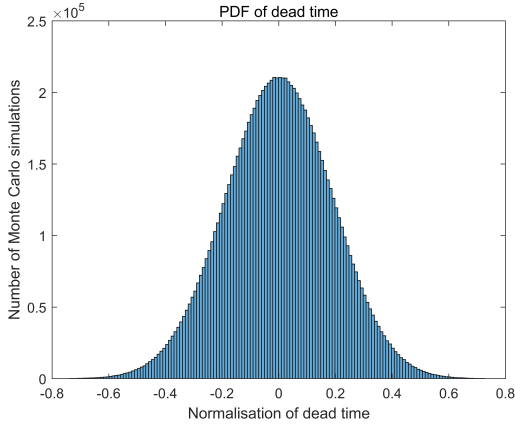

Fig. 6. Normalized histogram of the probability distribution function (PDF) of the system dead time by the MCM.

Finally, the value of E_n was used to determine whether the results of the two methods were consistent within the uncertainties. The E_n value is a statistical index used to evaluate the measurement capability of a laboratory. It is used to compare the difference between the laboratory measurement results and the reference value, as well as the measurement uncertainty. The closer the value of E_n is to zero, the closer the laboratory measurement results are to the reference values. If the absolute value of E_n is less than 1, the laboratory measurement results are considered consistent with the reference value. If the absolute value of E_n is greater than or equal

to 1, it is considered that the laboratory measurement results are inconsistent with the reference value. The formula for calculating the value of E_n is shown in Equation (16), where U_G and U_M are the expanded uncertainties (k=2) of the two methods. The results are summarized in Table 13.

$$E_n = \frac{|E_G - E_M|}{\sqrt{U_G^2 + U_M^2}} \tag{16}$$

IV. DISCUSSION

In the GUM and MCM methods, the system dead-time measurement model and voltage threshold correction factor measurement methods were the same, but the uncertainty evaluation methods were different. Only the β-plane source must complete the voltage threshold correction factor measurement. The GUM method is based on a Type B evaluation of the uncertainty process, and the default probability distribution of the system dead time and threshold correction factors is rectangular. The MCM inputs the measurements from the system dead time measurement model and the voltage threshold correction factor measurement method into Equation (15), and the uncertainty results of the system dead time and voltage threshold correction factor can be obtained through the Monte Carlo procedure. Thus, the final combined standard uncertainty can be calculated directly. It should be noted that in the MCM, the probability distribution of the threshold voltage readings is set to a rectangular distribution according to the Type B evaluation of uncertainty; however, in reality, the range of the coverage interval of the threshold voltage readings is much smaller than the scale component value (0.02 V).
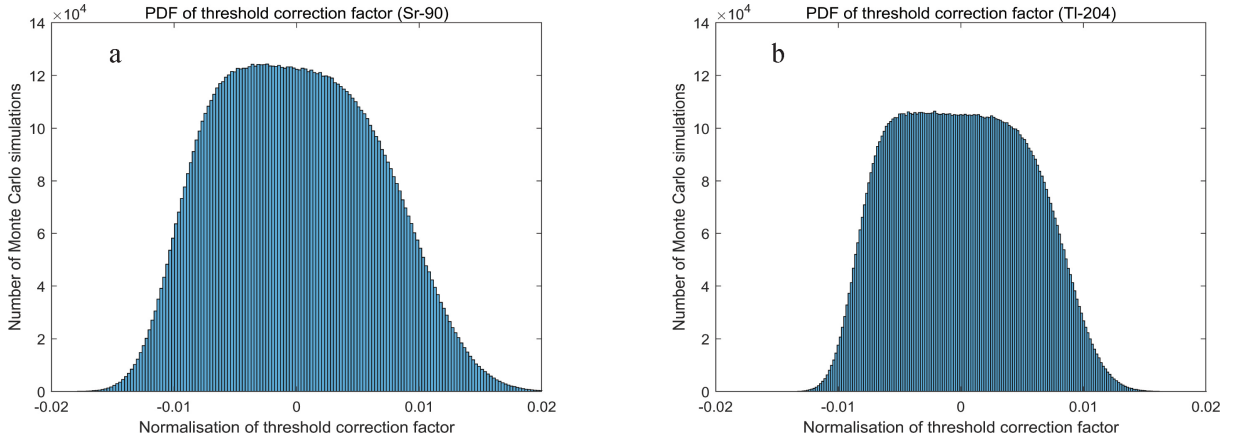
As can be observed from the evaluation results of the GUM and MCM methods, the system dead time and voltage threshold correction factor obtained by the MCM were similar to those of the GUM method; however, their measurement uncertainties were larger than those of the GUM method. Similarly, the final measurement estimates of the GUM and MCM methods for each source were similar. However, the uncertainty results of the MCM method were larger than those of

TABLE 6. Voltage threshold correction factors and coverage intervals at a threshold of 0.10 V.

β sources	q (s^{-1})	$px_1 + q$ (s^{-1})	Standard deviation, $px_1 + q$ (s^{-1})	Coverage interval, $px_1 + q$ (s^{-1})	f_d	Coverage interval, f_d
^{90}Sr	2124.44	2025.47	1.55	[2023.91,2027.02]	1.04887	[1.04806,1.04967]
^{204}Tl	2839.67	2723.61	1.33	[2722.28,2724.94]	1.04261	[1.04210,1.04312]

TABLE 7. Voltage threshold correction factors and their uncertainties for ^{90}Sr and ^{204}Tl of the GUM method

β sources	f_d	Standard uncertainty
^{90}Sr	1.0489	0.00047
^{204}Tl	1.0426	0.00030

Fig. 7. Normalized histograms of the PDF of the voltage threshold correction factors for the two β sources (^{90}Sr and ^{204}Tl) by the MCM.

the GUM method. This can be attributed to two reasons: (i) the combined standard uncertainty formula of the GUM method ignores the higher-order terms of the Taylor expansion in the process of partial derivation of the measurement model and (ii) the GUM method assumes that the probability distributions of the system dead time and voltage threshold correction factor have a rectangular distribution, which is more complex for both. Both reasons affected the evaluation results; however, the author believes that the second reason has more weight.

Compared to the GUM method, the MCM has unique advantages: the PDF of the output quantity Y can be output by the MCM, and the degree of discreteness of the output value can be observed. From the seven PDF histograms, it can be directly observed that (i) the probability distribution of the system dead time tends to be normally distributed, but the degree of discreteness is high, (ii) the probability distribution of the voltage threshold correction factors of the two β sources has a trapezoidal distribution characteristic, and (iii) it can be intuitively inferred from the PDFs of the four sources that the PDFs of ^{90}Sr have the highest degree of dispersion.

To improve the measurement method, it is recommended to use a digital multichannel analysis measurement system to obtain the system dead time directly by measuring the live time. Additionally, for a complete measurement system, performance tests, such as stability and repeatability, should also

be conducted.

V. CONCLUSION

In this study, methods for evaluating the uncertainty of α and β surface emission rate measurement models based on windowless proportional counters were studied using the GUM and MCM methods. The measurement methods and models of the system dead time and threshold correction factor were elaborated in detail, and the uncertainties of the surface emission rates of the four plane sources were evaluated using both the GUM and MCM methods.

The evaluation results of the GUM method were lower than those of the MCM method. However, the MCM method is considered to be more objective in its evaluation process and can better reflect the distribution characteristics of the surface emission rate measurement function through PDF graphs. To measure and calibrate the surface emission rate for α and β particles, the MCM constructs a mathematical model that is practical for stable environmental conditions and measurement methods in laboratories. The GUM method has greater flexibility in setting the coverage intervals of the measured quantities, whereas the MCM is more suitable for on-site calibration. Both methods can be used to validate the evaluation results.

TABLE 8. Values and relative standard uncertainties of the measured surface emission rate of the four plane sources based on the GUM method

Sources	E/s^{-1}	B/s^{-1}	R/s^{-1}	f_d	τ/s	$u_{\text{rel}}(B)$	$u_{\text{rel}}(R)$	$u_{\text{rel}}(f_d)$	$u_{\text{rel}}(\tau)$
^{241}Am	5514.70	0.608	5403.96	1	3.696×10^{-6}	15.57%	0.23%	0.000%	3.12%
^{239}Pu	5333.47	0.608	5229.78	1	3.696×10^{-6}	15.57%	0.50%	0.000%	3.12%
^{90}Sr	2098.93	39.46	2025.47	1.0489	3.696×10^{-6}	1.15%	0.18%	0.044%	3.12%
^{204}Tl	2827.70	39.46	2723.61	1.0426	3.696×10^{-6}	1.15%	0.32%	0.028%	3.12%

TABLE 9. Surface emission rate and combined standard uncertainties for the four plane sources of the GUM method

Sources	Surface emission rate $(E_G)/\text{s}^{-1}$	Standard uncertainty $(u_G)/\text{s}^{-1}$	Relative standard uncertainty $(u_{\text{rel-G}})$
^{241}Am	5514.7	13.9	0.25%
^{239}Pu	5333.5	27.9	0.52%
^{90}Sr	2098.9	4.5	0.22%
^{204}Tl	2827.7	10.4	0.37%

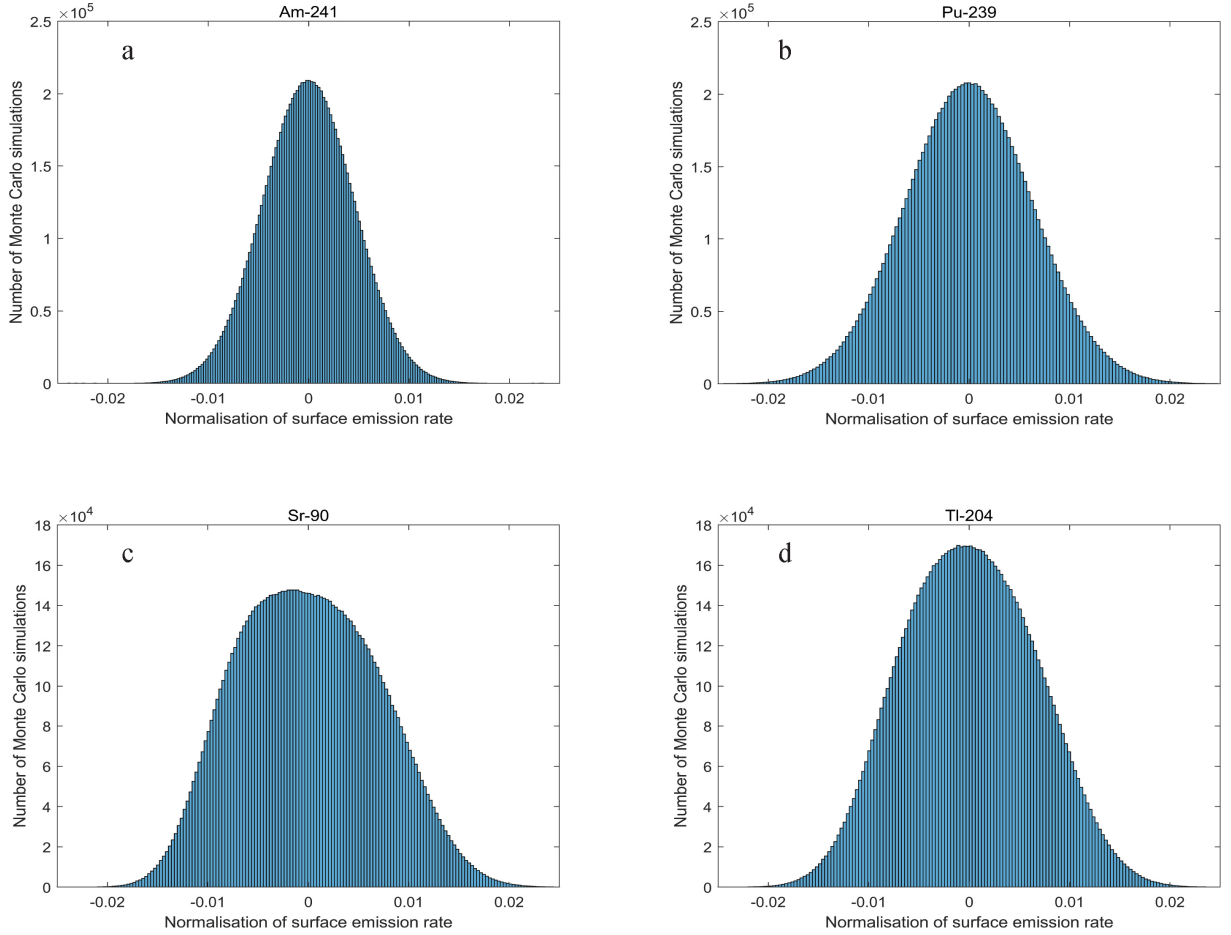Fig. 8. Normalized histogram of the PDF of the surface emission rate for the four sources (^{241}Am, ^{239}Pu, ^{90}Sr, ^{204}Tl) by the MCM .

TABLE 10. System dead time and its uncertainty with the MCM

Dead time (s)	Standard uncertainty (s)
3.694×10^{-6}	0.697×10^{-6}

TABLE 11. Voltage threshold correction factors and their uncertainties for ^{90}Sr and ^{204}Tlof the MCM

β sources	f_d	Standard uncertainty
^{90}Sr	1.0489	0.0047
^{204}Tl	1.0426	0.0055

TABLE 12. Surface emission rate and combined standard uncertainties for the four plane sources of the MCM

Sources	Surface emission rate (E_M) /s^{-1}	Standard uncertainty (u_M)/s^{-1}	Relative standard uncertainty ($u_{\text{rel-G}}$)
^{241}Am	5513.5	24.9	0.45%
^{239}Pu	5332.3	33.6	0.63%
^{90}Sr	2101.0	14.6	0.69%
^{204}Tl	2829.1	18.6	0.66%

[1] International Organization for Standards, *Reference sources — calibration of surface contamination monitors — alpha-, beta- and photon emitters.* (Geneva, Switzerland, 2018). ISO 8769.

[2] International Organization for Standards, *Measurement of radioactivity — Measurement and evaluation of surface contamination.* (Geneva, Switzerland, 2016). ISO 7503.

[3] F.D. Tang, L.F. He, Zhao, G.K et al., *Verification Regulation of Alpha and Beta Surface Contamination Instruments*, (Beijing, China, 2016).

[4] F.D. Tang, L.F. He, G.C. Liang et al., *Calibration Specification for α/β Planes Sources*, (Beijing, China, 2018).

[5] P. De. Felice, R. Anuradha, J. Bludovsky et al., Supplementary comparison of the measurement of the alpha and beta particle surface emission rates from large area sources (CCRI(II)-S10 LASCE), Metro. **59**, 1A (2022). https://doi.org/10.1088/0026-1394/59/1A/06007

[6] M. Unterweger, P. De Felice, Uncertainties in surface emission rate measurements, Metro. **52**, S165-S171 (2015). https://doi.org/10.1088/0026-1394/52/3/S165

[7] J.C. Liang, Q. Li, J.C. Liu et al., The absolute measurement for 2 and 2 particle emission rate. Acta Metrologica Sinica **37**, 209-213 (2016) (in Chinese). http://doi.org/10.3969/j.issn.1000-1158.2016.02.22

[8] J.L. Wuu, M.C. Yuan, S.H. Su et al., The alpha and beta emitter measurement system in INER. Appl. Radiat. Isot. **56**, 261-264 (2002). https://doi.org/10.1016/S0969-8043(01)00197-X

[9] Z.X. Li, H.J. He, J.C. Liang et al., The establishment of the on-site calibration device for 2 and 2 particle emission rate measurement. Acta Metrologica Sinica **38,** 117-122 (2017) (in Chinese). https://doi.org/10.3969/j.issn.1000-1158.2017.01.25

[10] International Organization for Standards, *Uncertainty of measurement-Part 3: Guide to the expression of uncertainty in measurement.* (Geneva, Switzerland, 2008). ISO/IEC GUIDE 98-3:2008(E).

[11] International Organization for Standards, *Uncertainty of measurement-Part 3: Guide to the expression of uncertainty in measurement- Supplement 1: Propagation of distributions using a Monte Carlo method.* (Geneva, Switzerland, 2008). ISO/IEC GUIDE 98-3:2008/Suppl.1.

[12] H. Sakai, T. Yoshii, A. Yunoki, Influence of conversion factors on the radioactivity evaluation of clearance objects consisting of several materials, Appl. Radiat. Isot **200**, 110984 (2023). https://doi.org/10.1016/j.apradiso.2023.110984

[13] H. Sakai, T. Yoshii, A. Yunoki, Evaluation of the probability distribution of radioactivity estimated by inverse problem solution using Monte Carlo Method, Appl. Radiat. Isot. **187**, 110338 (2022). https://doi.org/10.1016/j.apradiso.2022.110338

[14] Y. Xu, F. Gao, K.D. Wei et al., Simulation study on the fraction of environmental scattered radiation in mobile X-ray reference radiation field. NUCLEAR TECHNIQUES **44**, 3-11(2021) (in Chinese). https://10.11889/j.0253-3219.2021.hjs.44.100201.

[15] M. Lin, H. Ye, L. Xu et al., Test of proportional counter system with effective detective area larger than 1000 cm^2. Atomic Energy Science and Technology **50**, 713-719 (2016). (in Chinese). https://doi.org/10.7538/yzk.2016.50.04.0713

[16] S. Pommé, R. Fitzgerald, J. Keightley, Uncertainty of nuclear counting, Metro. **52**, S3-S17 (2015). https://doi.org/10.1088/0026-1394/52/3/S3

[17] M. Arkani, G. Raisali, Measurement of dead time by time interval distribution method. Nucl. Instrum. Methods Phys. Res. Sect. A **774**, 151-158 (2015). https://doi.org/10.1016/j.nima.2014.11.069

[18] E. Gilad, C. Dubi, B. Geslot et al., Dead time corrections using the backward extrapolation method. Nucl. Instrum. Methods Phys. Res. Sect. A **854**, 53-60 (2017). https://doi.org/10.1016/j.nima.2017.02.026

[19] L.C. Tian, Z.J. Zhao, Z. Chen et al., Simulation of a novel neutron detector based on multi-layer MWPC with ^{10}B$_4$C convertor. Nuclear Physics Review **36**, 71-77 (2019) (in Chinese). https://doi.org/10.11804/NuclPhysRev.36.01.071

[20] Q. Huang, F. Fang, Y. Yang et al., Research on repetition unit value for secondary standard of 2 and 2 particle emission rate. Nuclear Electronics & Detection Technology **32**, 471-474 (2012) (in Chinese). https://doi.org/10.3969/j.issn.0258-0934.2012.04.023

[21] J. Zhang, M. Zhang, L. Duan et al., The large-area multi-wire proportional counting system for 2 alpha and beta emission measurement at the NIM China. Appl. Radiat. Isot. **134**, 366-369 (2018). https://doi.org/10.1016/j.apradiso.2017.08.014

[22] Y.Q. Li, R.S. Wang, M. Zhang et al., Gas pressure dependence in the multi-wire proportional counter on the absolute measurement for and sources surface emission rates. Acta Metrologica Sinica **40**, 153-158 (2019) (in Chinese). https://doi.org/10.3969/j.issn.1000-1158.2019.01.25

[23] J. Hutchinson, Particle Counting in Radioactivity Measurements (ICRU Report 52), Metro. **32**, 326 (1995). https://doi.org/10.1088/0026-1394/32/4/15

TABLE 13. Comparison of results of GUM and MCM methods

Sources	E_n
^{241}Am	0.021
^{239}Pu	0.014
^{90}Sr	0.069
^{204}Tl	0.033

[24] A. Yunoki, Y. Hino, APMP comparison of measurement of surface emission rate of ^{36}Cl large area. Appl. Radiat. Isot. **70**, 1831-1835 (2012). https://doi.org/10.1016/j.apradiso.2012.02.034

[25] H.J. He, Z.X. Li, J.C. Liang et al., The development of a portable 2 particle emission rate measurement system. Nuclear Electronics & Detection Technology **36**, 1172-1177 (2016) (in Chinese). https://doi.org/10.3969/j.issn.0258-0934.2016.11.021

[26] Z. Tu, K.Z. Song, M. Zhang et al., A new digital pulse processing method for 2 and 2 emitter measurement. Nucl. Sci. Tech. **27**, 138 (2016). https://doi.org/10.1007/s41365-016-0137-z

[27] S. H. HWANG, J. M. LEE, K. B. LEE et al., Development of a windowless multi-wire proportional chamber (MWPC) counting system for measuring extended-area beta source. Appl. Radiat. Isot. **126**, 175-178 (2017). https://doi.org/10.1016/j.apradiso.2017.01.031

[28] L. E. KING, J. M. HUTCHINSON, M. P. UNTERWEGER, A new large-area 2π proportional counting system at NIST. Appl. Radiat. Isot. **66,** 877-880 (2008). https://doi.org/10.1016/j.apradiso.2008.02.079

[29] O. Helene, L. Mariano, Z.G. Filho, Useful and little-known applications of the Least Square Method and some consequences of covariances. Nucl. Instrum. Methods Phys. Res. Sect. A **833**, 82-87 (2016). https://doi.org/10.1016/j.nima.2016.06.126

[30] W. M. Sun, Simultaneous least-squares treatment of statistical and systematic uncertainties. Nucl. Instrum. Methods Phys. Res. Sect. A **556**, 325-330 (2006). https://doi.org/10.1016/j.nima.2005.10.030

[31] G. Schnabel, H. Leeb, A modified Generalized Least Squares method for large scale nuclear data evaluation. Nucl. Instrum. Methods Phys. Res. Sect. A **841**, 87-96 (2017). https://doi.org/10.1016/j.nima.2016.10.006

[32] H. Dembinski, M. Schmelling, R. Waldi, Application of the iterated weighted least-squares fit to counting experiments. Nucl. Instrum. Methods Phys. Res. Sect. A **940**, 135-141 (2019). https://doi.org/10.1016/j.nima.2019.05.086

[33] A. Baeza, L.M. Del Rio, C. Miro et al., Determination of ^{89}Sr and ^{90}Sr radioactive concentrations from least-squares fits to the growth/decay curves. Nucl. Instrum. Methods Phys. Res. Sect. A **312**, 198-200 (1992). https://doi.org/10.1016/0168-9002(92)90153-U

[34] J. Han, K.B. Lee, J. M. Lee et al., New method to incorporate Type B uncertainty into least-squares procedures in radionuclide metrology. Appl. Radiat. Isot **109**, 82-84 (2016). https://doi.org/10.1016/j.apradiso.2015.11.069

[35] H. Sakai, T. Yoshii, S. Kawasaki, Derivation of uncertainty propagation for clearance measurement. Appl. Radiat. Isot **170**, 109630 (2021). https://doi.org/10.1016/j.apradiso.2021.109630

[36] R. Michel, Measuring, Estimating, and Deciding under Uncertainty. Appl. Radiat. Isot **109**, 6-11 (2016). https://doi.org/10.1016/j.apradiso.2015.12.013

[37] D. Stanga a, P. De Felice, Improvements in the absolute standardization of large-area reference sources, Appl. Radiat. Isot. **67**, 1716-1720 (2009). https://doi.org/10.1016/j.apradiso.2009.03.056